Analyst

Accepted Manuscript

This article can be cited before page numbers have been issued, to do this please use: X. Gan, H. Zhao, S. Chen and X. Quan, *Analyst*, 2015, DOI: 10.1039/C5AN00082C.

ROYAL SOCIETY OF CHEMISTRY

www.rsc.org/analyst

View Article Online
DOI: 10.1039/C5AN00082C

Electrochemical DNA Sensor for Specific Detection of Picomolar Hg (Ⅱ) Based on Exonuclease Ⅲ- assisted Recycling Signal Amplification

Xiaorong Gan, Huimin Zhao*, Shuo Chen, Xie Quan

An ultrasensitive methodology was successfully developed for quantitative detection of picomolar Hg^{2+} based on the combination of the thymine-Hg^{2+}-thymine (T-Hg^{2+}-T) coordination chemistry and the Exonuclease III -aided recycling signal amplification. Single-strand probe DNA was immobilized on an Au electrode via the Au-S bond. In the presence of Hg^{2+}, the probe DNA would hybridize with the target DNA of four thymine-thymine (T-T) mismatches via the Hg^{2+}-mediated coordination of T-Hg^{2+}-T base pairs. Then the probe DNA in DNA duplex would be specifically recognized and selectively digested by Exonuclease III, in contrast the target DNA would be safely dissociated from DNA duplexes to continuously hybridize with a new signal probe, leading to the target recycling and signal amplification. As a result, the peak currents caused by the electrostatic interactions of $[Ru(NH_3)_6]^{3+}$ cations onto the backbone of probe DNA would decrease with different degrees corresponding to the Hg^{2+} concentrations. Under the optimum conditions, the proposed electrochemical DNA biosensor showed a robust detection limit as low as 1 pM (S/N=3), with a wide linear range from 0.01 to 500 nM and a good selectivity. In addition, the proposed method was successfully applied to assay Hg^{2+} in real environmental samples.

View Article Online
DOI: 10.1039/C5AN00082C

1. Introduction

Mercuric ion (Hg^{2+}), as a bioaccumulative and highly toxic environmental pollutant, can cause a lot of server and permanent damage on tissues and organs.[1] Especially, the Hg^{2+} ions in contaminated natural water can be indirectly intaken and accumulated by a food chain, which are difficult to be excreted by the metabolic system.[2] With respect to the toxicology and cellular effects, it was reported that even relatively low concentration of Hg^{2+} would result in the genotoxic effects if the human body suffered from chronic exposure. Therefore, it is still desirable and necessary to develop novel detection methods that could not only further improve the detection sensitivity and selectivity, but also be simple and environmentally friendly.

Traditional methods for Hg^{2+} detection, such as atomic absorption/emission spectroscopy,[3, 4] fluorimetry,[5, 6] inductively coupled plasma mass spectrometry,[7] and X-ray absorption spectroscopy,[8] are somewhat time-consuming in sample pretreatment and need sophisticated instrumentation skills.[9] Recently, several emerging sensor systems have been developed for Hg^{2+} detection,[2, 5, 6, 10-13] and some of sensors displayed satisfactory detection limit. For example, Yue et al.[11] reported a reusable biosensor for detecting mercury (II) based on ‘‘turn-on’’ resonance light scattering, and its detection limit was as low as 500 fM (S/N = 3). However, the above sensors were focused on the optical detection techniques which were strongly depended on sophisticated instruments and strict manipulation.[14]

Electrochemical biosensors,[15] as most promising candidate technologies, show many advantages in detecting Hg^{2+} because of simple instrumentation, less time

View Article Online
DOI: 10.1039/C5AN00082C

consumption, and real-time detection in situ.[16] In particular, the intrinsic specific interaction of thymine-thymine (T-T) mismatches can form T-Hg^{2+}-T base pairs in the presence of Hg^{2+}, which paved a promising avenue for developing the electrochemical biosensors with high stability to selectively detect trace or ultra-trace Hg^{2+}.[17] To this end, some strategies, such as nanomaterials,[12,14,18] enzymes[19,20] and structure-switching DNA[21-23] for signal simplification, have been employed in electrochemical biosensors to improve the sensitivity. Thereinto, enzymes, owing to the high specificity for their substrate molecule, have been extensively employed to construct enzyme-based biosensors in a wide range of analysis for the food and environment safety.[24] However, to the best of our knowledge, electrochemical biosensors based on the enzyme-amplified strategy for Hg^{2+} detection were rarely reported. The reported enzymes mainly included urease,[19] streptavidin-horseradish peroxidase (HRP)[20] and Exonuclease III (Exo III)[23].

Compared with urease and HRP, the unique properties of Exo III lie in consecutively catalyzing the stepwise removal of mononucleotides from 3'-hydroxyl termini of DNA duplexes with 3'-blunt or recessed, but its activity is limited on single-stranded DNA or 3'-overhang DNA duplexes with at least four bases long.[25, 26] Therefore, the Exo III will possess a high potential for applications in constructing electrochemical DNA (E-DNA) sensors. In view of the above properties of Exo III, an E-DNA sensor based on the conformational change of the probe and Exo III's activity on DNA hybrids containing T-Hg^{2+}-T base pairs was proposed for Hg^{2+} detection[23]. In that strategy, under the presence of Hg^{2+} a thymine-rich DNA oligonucleotide (e-T-rich

View Article Online
DOI: 10.1039/C5AN00082C

probe) exhibited a conformational conversion from the linear e-T-rich probe into a hairpin structure by T-Hg^{2+}-T base pair. The DNA duplexes with hairpin structure activated the Exo III which resulted in the stepwise removal of mononucleotides from the 3'terminus of the e-T-rich probe and the release of a thymidine monophosphate with the methylene blue (MB) tag. Because the electrostatic repulsion between the MB tag and the negative ITO electrode surface was smaller than that between the e-T-rich probe and the negative ITO electrode surface. The released MB tag led to a distinct increase in the electrochemical signal, which was used to construct the E-DNA sensor for monitoring Hg^{2+} with a detection limit of 0.2 nM[23].

Recently, it was reported that the Exo III has also been employed to construct electrochemical biosensors for detecting femtomolar DNA by DNA hybridization [25-27]. Therefore, it is still possible to improve the detection limit of Hg^{2+} by constructing an E-DNA sensor based on the Exo III's activity. Bearing this fact in mind, we took advantage of the Exo III - assisted recycling signal amplification and the specific molecular recognition function towards Hg^{2+} from T-T mismatched bases to fabricate a rapid, high selective and ultrasensitive E-DNA sensor for Hg^{2+} detection. Compared with the reported E-DNA sensor based on Exo III for Hg^{2+} detection[23], in this study single-strand probe DNA was directly immobilized on an Au electrode by the Au-S bond. In addition, the electrical signals were generated by the redox reaction of RuHex molecules onto the phosphates backbone of probe DNA owing to the electrostatic interaction. The experiment results showed that our proposed E-DNA sensor not only exhibited a high selectivity, but also displayed a robust limit detection

View Article Online
DOI: 10.1039/C5AN00082C

of 1 pM (S/N=3), which greatly improved the sensitivity of current electrochemical biosensors based on the enzyme-amplified strategy.

2. Materials and methods

2.1. Chemical reagents

DNA oligonucleotides (probe DNA, FAM-modified probe DNA and target DNA), Exo III and 10×Exo III buffer were purchased from by TaKaRa Biotech. Co., Ltd. (Dalian, China).

The probe DNA was modified at the 5'-end with a sulfhydryl modifier (5'- SH -$(CH_2)_6$-GAT-TCC-GTG-CAT-GAC-TCA-G-3').

The target DNA was four-base mismatch to the probe DNA (4-Mis DNA: 5'-C-TGT-GTC-TTG-CTC-GGT-ATC-AAGCG-3').

The FAM-modified probe DNA with the following sequence: 5'- SH -$(CH_2)_6$-GAT-TCC-GTG-CAT-GAC-TCA-G- FAM -3', was used to repeat the same experiments.

The length of target DNA was designed according to the conclusion: the optimal 3'-overhang length in the duplex structure should be at least four bases so that the degradation of target DNA by Exo III can be avoided.[26] Hexaammineruthenium (III) chloride ($Ru(NH_3)_6^{3+}$, RuHex), tris (2-carboxyethyl) phosphine hydrochloride (TCEP) and 6-Mercapto-1-hexanol (MCH) were provided by Aladdin Industrial Corporation (Shanghai, China). All other chemicals were purchased from Tianjin Kemiou Chemical Reagent Co., Ltd., and were of analytical grade without additional

View Article Online
DOI: 10.1039/C5AN00082C

purification. All solutions were prepared with ultrapure water (Milli-Q water, 18.2 MΩ cm) from a Millipore Milli-Q system (Bedford, MA, USA).

The buffers used here were as follows: probe DNA immobilization buffer (Buffer-1) was 0.1 M NaCl, 10 μM TCEP and 10 mM Tris-HCl (pH=7.4); MCH incubation buffer (Buffer-2) was 5 mM MCH and 10 mM Tris-HCl (pH=7.4); Exo III incubation buffer (Buffer-3) was 50 mM Tris-HCl (pH=8), 5 mM $MgCl_2$, 1 mM DL-Dithiothreitol (DTT), 1 μM target DNA, 1.8 units/μL Exo III and 0.4 M NaCl (Fig. S1, Supporting Information). All electrochemical characterizations including square-wave voltammograms (SWV), cyclic voltammograms (CV) and electrochemical impedance spectroscopy (EIS) were carried out on CHI 660D electrochemical workstation (Shanghai, China) at laboratory ambient room temperature (RT, 22-25℃). The three-electrode electrochemical cell consisted of a bare gold working electrode (2 mm in diameter), a platinum counter electrode and a saturated calomel electrode (SCE) as reference electrode (saturated with 3.0 M KCl). The fluorescence spectroscopy was obtained by fluorescence spectrophotometer (F-4500, Hitach).

2.2. Fabrication of probe DNA-modified Au electrode

The probe DNA-modified Au electrode was fabricated according to a procedure previously described elsewhere.[28, 29] Briefly, a bare gold electrode was polished in sequence with alumina suspensions of 1, 0.3 and 0.05 μm diameter. Afterwards, the electrode was sonicated in absolute ethanol and ultrapure water for 5 min two times in

View Article Online
DOI: 10.1039/C5AN00082C

turn to remove the possible bound microparticles. Then the electrode was immersed in piranha solution (H_2SO_4/H_2O_2=3:1 in volume) for 0.5 h to eliminate the adsorbed organics. Sequently, the electrode was subjected to the continuous potential cycling (-0.3−1.5 V, 50 mV/s) in 0.50 M aqueous H_2SO_4 until cyclic voltammograms became reproducible. After that, the as-formed clean gold electrode can be confirmed by a cyclic voltammogram characteristic (Fig. S2, Supporting Information). Finally, the electrode was washed thoroughly with ultrapure water and dried in N_2; immediately, 10 μL probe DNA (1 μM) dissolved in Buffer-1 was dropped onto the clear electrode and then kept at 4□ for 24 h. After that, the electrode was gently immersed in 10 mM Tris-HCl (pH=7.4) for 5-10 s to remove the unbound probe DNA, followed by a 2 h exposure in Buffer-2 to prevent nonspecific probe DNA adsorption on the surface of gold and blow-dry with nitrogen.

2.3 Electrochemical detection of Hg^{2+}

In order to detect Hg^{2+}, the probe DNA-modified Au electrodes were immersed in Buffer-3 with a series of different concentrations of Hg^{2+} (0-10 μM) and kept at 37 ℃ for 30 min and then heated to 65 °C for 5 min to inactivate Exo III and stop the digestion reaction. Finally the electrodes were gently immersed in 10 mM Tris-HCl (pH=7.4) for 5-10 s to remove DNA fragments after digestion and then immersed in 10 mM Tris-HCl (pH=7.0) with 50 μM RuHex to obtain the final redox currents by SWV measurements. The parameters of SWV measurement were as follows: initial potential of -0.6 V, final potential of 0 V, frequency of 25 Hz. Of note, prior to detect

View Article Online
DOI: 10.1039/C5AN00082C

Hg^{2+}, the electrodes underwent SWV and EIS measurements in 0.1 M KCl solution containing 2.5 mM $K_3[Fe(CN)_6]$ and 2.5 mM $K_4[Fe(CN)_6]$ in the frequency range from 0.001 to 100 kHz with 5 mV as the amplitude. In addition, CV was employed to test the changes of RuHex redox current in 10 mM Tri-HCl (pH=7.4) containing 10 μM $[Ru(NH_3)_6]^{3+}$ solution before and after Hg^{2+} detection within the potential range from -0.7 to 0 V at a scan rate of 50 mV/s.

3. Results and discussion

3.1 Design strategy of E-DNA sensor

As depicted in Scheme 1, first of all, probe DNA with a thiol group at 5'end were covalently immobilized on an Au electrode. MCH as a spacer thiol was employed to minimize the nonspecific adsorption of probe DNA for maximizing the hybridization efficiency, because MCH can lift the probe DNA from the surface and immobilize the probe DNA on the Au electrode solely through the thiolate.[30, 31] After the probe DNA modified Au electrode was exposed in Buffer-3 after adding various concentrations of Hg^{2+}, Hg^{2+} would be captured because the hybridization reaction was triggered between the probe DNA and the target DNA with four T-T mismatches via forming T-Hg^{2+}-T complexes. Afterwards, the hybridized DNA duplexes can be selectively digested by Exo III. Because of a 3'-blunt end at the probe DNA and a 3'-overhang end at the target DNA, the probe DNA would be digested, in contrast the target DNA would be safely dissociated from the double-strand DNA to continuously hybridize with other probe DNA for the next recycling process. After suffering from a sequence

View Article Online
DOI: 10.1039/C5AN00082C

of the hybridization and digestion processes, the electrode was finally immersed into the RuHex electrolyte solution to record the current changes with various concentrations of Hg^{2+}. Due to the strongly electrostatic binding, the signaling transducer RuHex cations would absorb strongly on the anionic phosphate backbones of DNA. Thus, the peak currents would be directly proportional to the amount of residual probe DNA. That is, the concentration of Hg^{2+} can be detected according to the current changes of RuHex in SWV measurements. Of note, the E-DNA sensor may show unique advantages for monitoring ultralow concentration of Hg^{2+} owing to the recycling or accumulation amplified effects of Exo □.

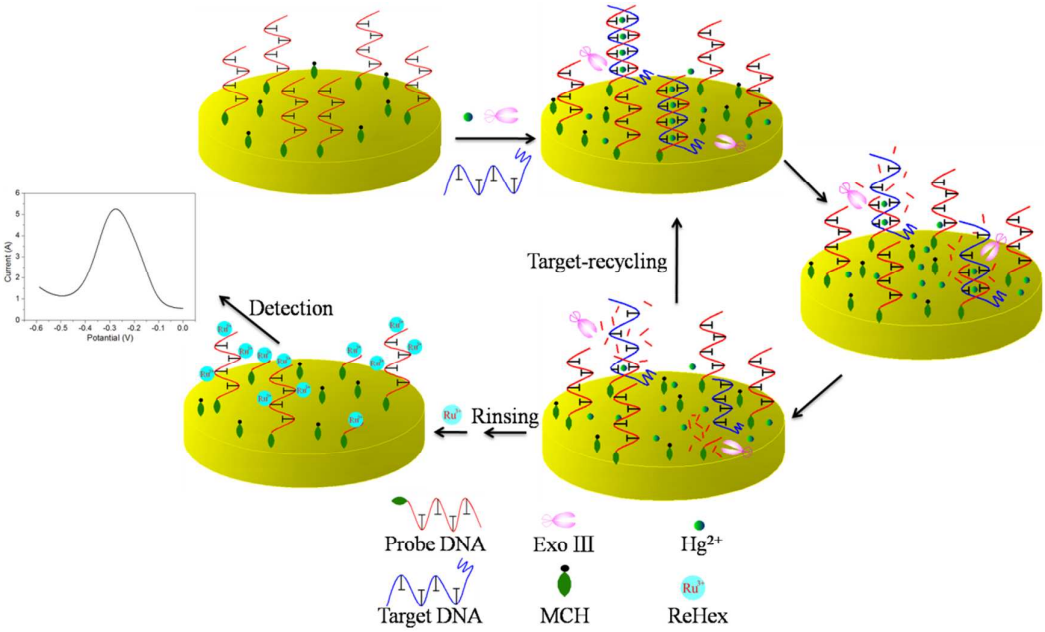

Scheme 1. Schematic representation of E-DNA sensor via Exo III-aided target recycling amplification for specific detection of Hg^{2+}.

View Article Online
DOI: 10.1039/C5AN00082C

3.2 Electrochemical characterization of E-DNA sensor

Cyclic voltammetry was employed to explore the electrochemical behavior of the Au electrode or the modified Au electrodes using RuHex as an electroactive probe. As shown in Fig. 1, no redox peaks can be observed at bare Au electrode in the potential range from -0.7 to 0 V.[32] In contrast, one couple of weak peaks appeared for the MCH modified-Au electrode, indicating little amounts of RuHex molecules were adsorbed onto the short alkanethiol.[26] The voltammogram of probe DNA-modified Au electrode exhibited a pair of well defined and symmetric redox peaks with the negligible peak separation at a scan rate of 50 mV/s. The phenomenon indicates that a large number of $[Ru(NH_3)_6]^{3+}$ molecules interacted electrostatically with the anionic phosphate of DNA backbone and the one-electron reduction of $[Ru(NH_3)_6]^{3+}$ to $[Ru(NH_3)_6]^{2+}$ was reversible.[31] The peak current of the probe DNA-modified Au electrode after assaying 10 μM Hg^{2+} was clearly decreased but still stronger than that of the MCH modified-Au electrode, demonstrating little amounts of residual probe DNA fragments tethered on the surface of the Au electrode after assaying 10 μM Hg^{2+} as shown in Scheme 1. In addition, a wide and weak peak can be observed at ~ -1.8 V for the probe DNA-modified Au electrode before and after assaying 10 μM Hg^{2+}, which may be ascribed to the absorption of reduced form $[Ru(NH_3)_6]^{2+}$.[33]

View Article Online
DOI: 10.1039/C5AN00082C

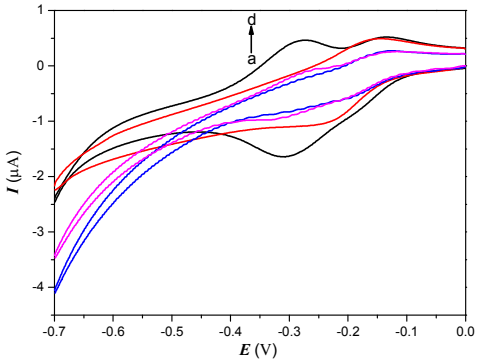

Fig. 1. Cyclic voltammograms of bare Au electrode (a), MCH modified-Au electrode (b), probe DNA-modified Au electrode after assaying 10 μM Hg^{2+} (c) and probe DNA-modified Au electrode (d) in 10 mM Tri-HCl (pH=7.4) containing 10 μM $[Ru(NH_3)_6]^{3+}$ solution at a scan rate of 50 mV/s.

In order to get a better insight into the electron-transfer behavior, EIS and SWV measurements were performed to characterize the modified Au electrodes by different interfacial processes. With respect to EIS, the length of semicircle diameter in Nyquist plot corresponds to the electron-transfer resistance. As depicted in Fig. 2A, the bare Au electrode displayed a straight line (curve a), which was the characteristic of an ideal conductor[21]. After modification with MCH, an obvious semicircle can be seen (curve b), suggesting that the electron transfer was hindered between ferricyanide (3-/4-) and the electrode surface because of the self-assembled monolayer of MCH; on the other hand, it implied that the Au electrode was successfully modified by MCH. Compared with the bare Au electrode or the MCH-modified Au electrode, the semicircle diameter of probe DNA-modified Au electrode after assaying 10 μM Hg^{2+} exhibited a slight increase (curve c). The result can be accounted for a certain amount of residue probe DNA on Au electrode, which was in good agreement with Fig. 1. Of note, the probe DNA modified Au electrode

View Article Online
DOI: 10.1039/C5AN00082C

greatly increased the obstacle of electron transfer (curve d). This should be ascribed to the electrostatic repulsion force between the negatively charged phosphate backbone of the oligonucleotides and ferricyanide (3-/4-).[27]

Correspondingly, from SWV curves shown in Fig. 2B, it can be seen that a remarkable peak displayed at ~-0.336 V in the case of probe DNA-modified Au electrode, and two peaks appeared at ~-0.248 V for the bare Au electrode and ~-0.196 V for the MCH-modified Au electrode, respectively. Furthermore, the peak currents significantly decreased for both the MCH-modified Au electrode and the probe DNA-modified Au electrode after assaying 10 μM Hg^{2+}. The aforementioned results suggested that the electron-transfer/exchange process was carried out through the phosphate backbone, even for long-range electron transfer.[34] In addition, the peak potentials of the probe DNA-modified Au electrode before and after assaying 10 μM Hg^{2+} changed a lot probably because the presence of probe DNA enhanced the electrode polarization effects.

View Article Online
DOI: 10.1039/C5AN00082C

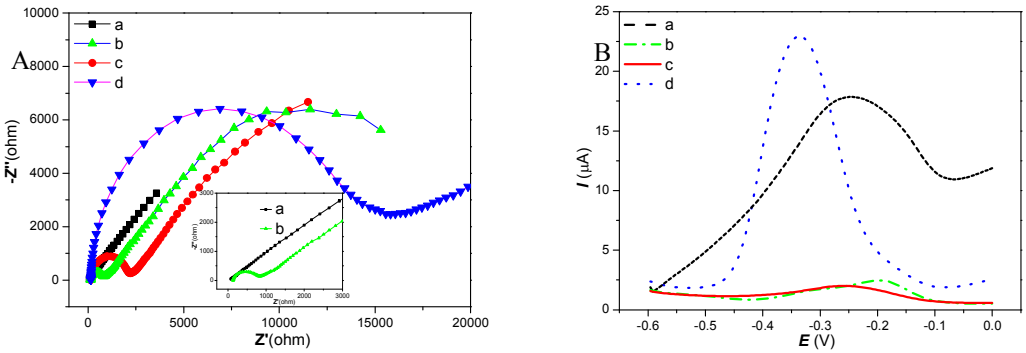

Fig. 2. (A) EIS in 0.1 M KCl solution containing 2.5 mM $K_3[Fe(CN)_6]$ and 2.5 mM $K_4[Fe(CN)_6]$ and (B) SWV curves in 10 mM Tris-HCl (pH=7.0) with 50 μM RuHex at bare Au electrode (a), MCH modified-Au electrode (b), probe DNA-modified Au electrode after assaying 10 μM Hg^{2+} (c) and probe DNA-modified Au electrode (d). The insets show larger version EIS plots of curves a and b.

3.3. Optimization of the experimental conditions

In order to obtain an ideal response to Hg^{2+}, the parameters including the concentrations of probe DNA and NaCl were optimized. Other parameters such as pH value, the reaction time and the reaction temperature of Exo III were set according to the enzyme specification reported previously.[35, 36] In this study, the concentration of probe DNA was determined as 1 μM according to the work of Ye group.[26] Therein, the Ye group reported the effects of the different surface densities on the hybridization efficiency of probe DNA and target DNA, and found that the reproducible maximum hybridization signaling can be obtained as 1 μM of probe DNA was employed to modify an Au electrode. In addition, the NaCl concentration in Buffer-3 can also affect the detection limit and the sensitivity. On one hand, the adsorption of probe DNA was greatly reduced at the low NaCl concentration[30]; on the other hand, the activity of Exo III was significantly inhibited at the high NaCl concentration.[37]

View Article Online
DOI: 10.1039/C5AN00082C

Therefore, different NaCl concentrations were investigated in the study. As shown in Fig. 1S, it can be seen that the peak current of RuHex for assaying 50 nM Hg^{2+} decreased as the NaCl concentration was changed from 0 to 0.4 M, reaching a maximum at 0.4 M, and then increased up from 0.4 to 1 M. Under same conditions, 0.4 M NaCl can ensure the best sensitivity of E-DNA sensor. Thus, 1 μM of probe DNA in Buffer-1 and 0.4 M NaCl in Buffer-3 were selected as the optimal parameters for Hg^{2+} detection.

3.4. Quantitative determination of Hg^{2+} by SWV

The sensitivity of E-DNA sensor was investigated by SWV responses to Hg^{2+} of varying concentrations under the optimal conditions. As shown in Fig. 3A, the SWV peak currents gradually decreased in the range from 0.002 nM to 10 μM with the increase of Hg^{2+} concentration. This phenomenon was consistent with the design strategy, which was caused by the diminished amount of probe DNA after suffering from the DNA hybridization and the Exo Ⅲ's digestion. In order to further confirm the above process, we used the FAM-modified probe DNA to investigate the relationship between the fluorescence intensity of Exo III's incubation buffer and the incubation time (Fig. S3, Supporting Information). It can be seen that the fluorescence intensity increased with the passing of time, indicating that the increased amount of probe DNA fragments labeled with the fluorescence group of FAM entered into the buffer solution owing to the Exo Ⅲ's digestion over time, which again certified our design routine.

View Article Online
DOI: 10.1039/C5AN00082C

Fig. 3B shows the relationship between SWV peak currents and Hg^{2+} concentrations. It was observed that the E-DNA sensor exhibited a linear range from 0.01 to 500 nM with a detection limit of 1 pM (3S/N) for Hg^{2+} detection, as depicted in Fig. 3C. The regression equation is I = 9.5955-2.6018 lg([Hg^{2+}]) with a correlation coefficient of 0.9993. To the best of our knowledge, such a low detection limit is rather impressive compared with the reported biosensors for Hg^{2+} detection (Table S1, Supporting Information). Therefore, the E-DNA sensor might have potential applications in environmental monitoring of the exposure of Hg^{2+}.

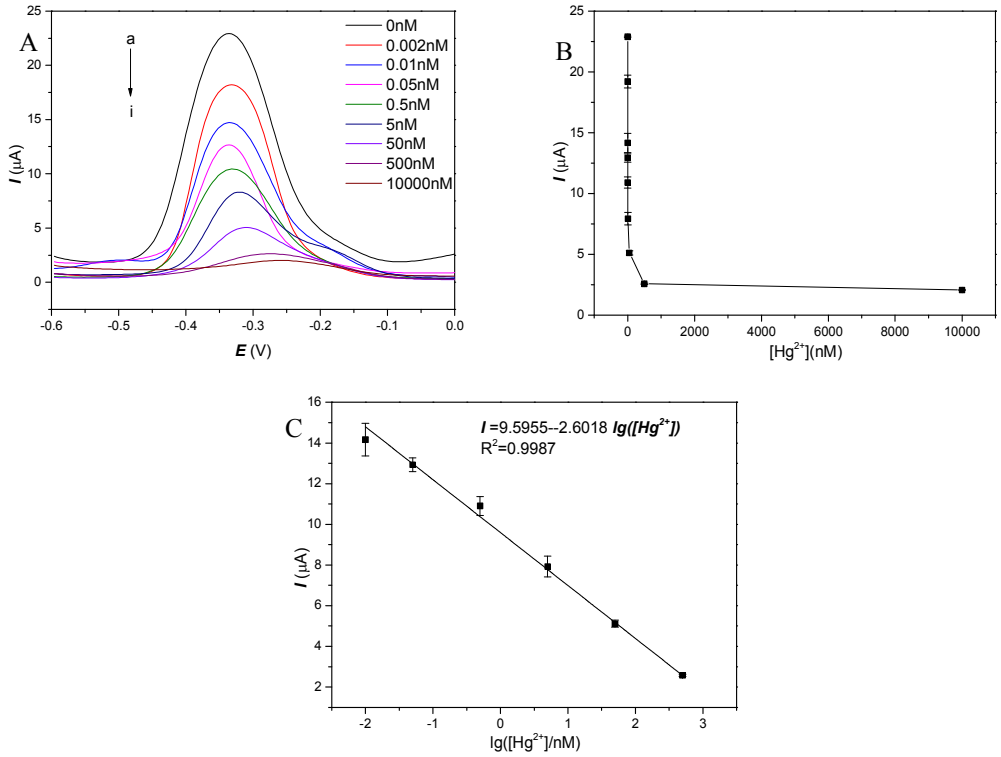

Fig. 3. (A) Typical SWV curves of the as-prepared E-DNA sensor in response to Hg^{2+} of varying concentrations, from 0 to 10 μM (a-i). (B) The plot of SWV peak currents vs Hg^{2+} concentrations. (C) Linear relationship between peak currents and the logarithm of Hg^{2+}

View Article Online
DOI: 10.1039/C5AN00082C

concentrations. Error bars are standard deviation across three repetitive experiments using three different electrodes.

3.5. Selectivity of E-DNA sensor

To explore the selectivity of the proposed E-DNA sensor, the influences of some other metal ions (Pb^{2+}, Ni^{2+}, Mn^{2+}, Zn^{2+}, Fe^{3+}, Cu^{2+}, K^{+}, Ag^{+}, Co^{2+}, Mg^{2+}, Cd^{2+}) on the determination of Hg^{2+} were investigated under identical conditions. As shown in Fig. 4, SWV peak currents decreased dramatically in response to Hg^{2+} at 10 μM but hardly exhibited substantial responses to other metal ions at same concentration. Moreover, the difference above was still significant even at 5 nM Hg^{2+} which is the limit amount of mercury ions in drinking water by the World Health Organization. This indicated that the proposed E-DNA sensor had an excellent selectivity to Hg^{2+} against other environmentally relevant meta ions. The excellent selectivity should be attributed to the specific coordination between T bases and Hg^{2+}.

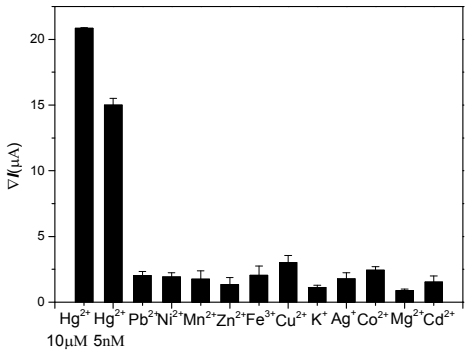

Fig.4. Normalized SWV peak currents of the proposed E-DNA sensor in responses to other metal ions (10 μM) and Hg^{2+}(10 μM and 5 nM)

View Article Online
DOI: 10.1039/C5AN00082C

3.6 Analysis of Hg^{2+} in real water samples

To demonstrate its versatility, the as-formed E-DNA sensor was applied in analysis of Hg^{2+} in tap water and Bajia river (Dalian, China). The samples firstly were filtered through 0.2 mm membrane to get rid of the insolubles for Hg^{2+} detection. The concentration of Hg^{2+} in tap water can not be detectable, therefore standard Hg^{2+} solutions with different concentrations were added in tap water. The results were summarized in Table 1. The recovery values and RSD values demonstrated the good accuracy and adaption of the proposed E-DNA sensor in detecting real samples. In particular, the sensor may be more adaptable for detecting the low-mercury water samples certified by a smaller RSD value in low concentration.

Table 1 Determination of Hg^{2+} in tap water and river

No.	Sample	Add	ICP-MS	E-DNA sensor	Recovery%	RSD% (n=3)
1	Bajia river		99.7nM	95.8nM	96.2	8.5
2	Tap water		non-detectable	non-detectable		
3	Spiked tap water 1	10 nM		11.1 nM	111.0	1.5
4	Spiked tap water 2	80 nM		73.9 nM	92.3	5.9

4. Conclusion

In summary, a novel electrochemical DNA sensor for ultrasensitive and selective detection of Hg^{2+} was developed by combining the T-Hg^{2+}-T coordination chemistry with the Exo III-aided target recycling strategy. Compared with other biosensors

View Article Online
DOI: 10.1039/C5AN00082C

based on the T-Hg^{2+}-T interaction, the detection limit was greatly lowered to 1 pM. Furthermore, the desirable performance can be easily realized via using the commercially available Au electrode, which facilitates the procedure for monitoring Hg^{2+} and avoids the tedious synthesis procedures of nanomaterials for signal amplification. Meanwhile, the developed method had also been demonstrated to be suitable for monitoring real samples. Even though this electrode is one-off, it is undeniable that this assay is high sensitive and selective for environmental monitoring of trace Hg^{2+}.

Acknowledgments

This study was supported by the National Natural Science Foundation of China (No. 21277016) and the Research Project of Chinese Ministry of Education (No. 113017A).

View Article Online
DOI: 10.1039/C5AN00082C

References

1 I. Bontidean, A. Mortari, S. Leth, N. L. Brown, U. Karlson, M. M. Larsen, J. Vangronsveld, P. Corbisier and E. Csoregi, Biosensors for detection of mercury in contaminated soils, *Environ. Pollut.*, 2004, **131**, 255-262.

2 C. J. Yu, T. L. Cheng and W. L. Tseng, Effects of Mn^{2+} on oligonucleotide-gold nanoparticle hybrids for colorimetric sensing of Hg^{2+}: improving colorimetric sensitivity and accelerating color change, *Biosens. Bioelectron.*, 2009, **25**, 204-210.

3 F. X. Han, W. D. Patterson, Y. Xia, B. B. M. Sridhar and Y. Su, Rapid determination of mercury in plant and soil samples using inductively coupled plasma atomic emission spectroscopy, a comparative study, *Water, Air, and Soil Pollution*, 2006, **170**, 161-171.

4 W. J. Suddendorf RF and K. Boyer, Simplified apparatus for determination of mercury by atomic absorption and inductively coupled plasma emission spectroscopy, *J. Assoc. Off. Anal. Chem.*, 1981, **64**, 1105-1110.

5 Y. Wang, F. Yang and X. Yang, Colorimetric biosensing of mercury (II) ion using unmodified gold nanoparticle probes and thrombin-binding aptamer, *Biosens. Bioelectron.*, 2010, **25**, 1994-1998.

6 B. C. Ye and B. C. Yin, Highly sensitive detection of mercury (II) ions by fluorescence polarization enhanced by gold nanoparticles, *Angew. Chem. Int. Ed. Engl.*, 2008, **47**, 8386-8389.

7 O. T. Butler, J. M. Cook, C. F. Harrington, S. J. Hill, J. Rieuwerts and D. L. Miles, Atomic spectrometry update. Environmental analysis, *J. Anal. At. Spectrom.*, 2007, **22**, 187-221.

8 A. Bernaus, X. Gaona, J. M. Esbri, P. Higueras, G. Falkenberg and M. Valiente, Microprobe techniques for speciation analysis and geochemical characterization of mine environments: the mercury district of almadén in Spain, *Environ. Sci. Technol.*, 2006, **40**, 4090-4095.

9 Q. Li, X. Zhou and D. Xing, Rapid and highly sensitive detection of mercury ion (Hg^{2+}) by magnetic beads-based electrochemiluminescence assay, *Biosens. Bioelectron.*, 2010, **26**, 859-862.

10 X. Xu, J. Wang, K. Jiao and X. Yang, Colorimetric detection of mercury ion (Hg^{2+}) based on DNA oligonucleotides and unmodified gold nanoparticles sensing system with a tunable detection range, *Biosens. Bioelectron.*, 2009, **24**, 3153-3158.

11 Q. L. Yue, T. F. Shen, J. T. Wang, L. Wang, S. L. Xu, H. B. Li and J. F. Liu, A reusable biosensor for detecting mercury (II) at the subpicomolar level based on "turn-on" resonance light scattering, *Chem.Comm.*, 2013, **49**, 1750-1752.

12 Y. Zhang, H. Zhao, Z. Wu, Y. Xue, X. Zhang, Y. He, X. Li and Z. Yuan, A novel graphene-DNA biosensor for selective detection of mercury ions, *Biosens. Bioelectron.*, 2013, **48**, 180-187.

13 Q. Liu, J. J. Peng, L. N. Sun and F. Y. Li, High-efficiency upconversion luminescent sensing and bioimaging of Hg (II) by chromophoric ruthenium

View Article Online
DOI: 10.1039/C5AN00082C

complex-assembled nanophosphors, *ACS Nano*, 2011, **5**, 8040-8048.

14 S. Tang, P. Tong, W. Lu, J. Chen, Z. Yan and L. Zhang, A novel label-free electrochemical sensor for Hg^{2+} based on the catalytic formation of metal nanoparticle, *Biosens. Bioelectron.*, 2014, **59**, 1-5.

15 A. Chen and S. Chatterjee, Nanomaterials based electrochemical sensors for biomedical applications, *Chem. Soc. Rev.*, 2013, **42**, 5425-5438.

16 D. Wei, M. J. Bailey, P. Andrew and T. Ryhanen, Electrochemical biosensors at the nanoscale, *Lab Chip*, 2009, **9**, 2123-2131.

17 Y. Miyake, H. Togashi, M. Tashiro, H. Yamaguchi, S. Oda, M. Kudo, Y. Tanaka, Y. Kondo, R. Sawa, T. Fujimoto, T. Machinami and A. Ono, Mercury (II)-mediated formation of thymine-Hg^{II}-thymine base pairs in DNA duplexes, *J. Am. Chem. Soc.*, 2006, **128**, 2172-2173.

18 D. T. Nguyen, L. D. Tran, H. L. Nguyen, B. H. Nguyen and N. V. Hieu, Modified interdigitated arrays by novel poly (1,8-diaminonaphthalene)/carbon nanotubes composite for selective detection of mercury (II), *Talanta*, 2011, **85**, 2445-2450.

19 O. Dominguez-Renedo, M. A. Alonso-Lomillo, L. Ferreira-Goncalves and M. J. Arcos-Martinez, Development of urease based amperometric biosensors for the inhibitive determination of Hg (II), *Talanta*, 2009, **79**, 1306-1310.

20 Z. P. Zhang, A. Tang, S. Z. Liao, P. F. Chen, Z. Y. Wu, G. L. Shen and R. Q. Yu, Oligonucleotide probes applied for sensitive enzyme-amplified electrochemical assay of mercury (II) ions, *Biosens. Bioelectron.*, 2011, **26**, 3320-3324.

21 D. Wu, Q. Zhang, X. Chu, H. Wang, G. Shen and R. Yu, Ultrasensitive electrochemical sensor for mercury (II) based on target-induced structure-switching DNA, *Biosens. Bioelectron.*, 2010, **25**, 1025-1031.

22 X. Niu, Y. Ding, C. Chen, H. Zhao and M. Lan, A novel electrochemical biosensor for Hg^{2+} determination based on Hg^{2+}-induced DNA hybridization, *Sensors and Actuators B: Chemical*, 2011, **158**, 383-387.

23 F. Xuan, X. T. Luo and I. M. Hsing, Conformation-dependent exonuclease III activity mediated by metal ions reshuffling on thymine-rich DNA duplexes for an ultrasensitive electrochemical method for Hg^{2+} detection, *Anal. Chem.,* 2013, **85**, 4586-4593.

24 A. Amine, H. Mohammadi, I. Bourais and G. Palleschi, Enzyme inhibition-based biosensors for food safety and environmental monitoring, *Biosens. Bioelectron.*, 2006, **21**, 1405-1423.

25 C. S. Lin, Y. F. Wu, F. Luo, D. M. Chen and X. Chen, A label-free electrochemical DNA sensor using methylene blue as redox indicator based on an exonuclease III-aided target recycling strategy, *Biosens. Bioelectron.*, 2014, **59**, 365-369.

26 D. Wu, B.C. Yin and B. C. Ye, A label-free electrochemical DNA sensor based on exonuclease III-aided target recycling strategy for sequence-specific detection of femtomolar DNA, *Biosens. Bioelectron.*, 2011, **28**, 232-238.

27 C. Luo, H. Tang, W. Cheng, L. Yan, D. Zhang, H. Ju and S. Ding, A sensitive electrochemical DNA biosensor for specific detection of Enterobacteriaceae bacteria by exonuclease III-assisted signal amplification, *Biosens. Bioelectron.,* 2013, **48**,

View Article Online
DOI: 10.1039/C5AN00082C

132-137.

28 Y. Xiao, R. Y. Lai and K. W. Plaxco, Preparation of electrode-immobilized, redox-modified oligonucleotides for electrochemical DNA and aptamer-based sensing, *Nat. Protoc.*, 2007, **2**, 2875-2880.

29 J. Zhang, S. P. Song, L. H. Wang, D. Pan and C. H. Fan, A gold nanoparticle-based chronocoulometric DNA sensor for amplified detection of DNA, *Nat. Protoc.*, 2007, **2**, 2888-2895.

30 T. M. Herne and M. J. Tarlov, Characterization of DNA probes immobilized on gold surfaces, *J. Am. Chem. Soc.*, 1997, **119**, 8916-8920.

31 A. B. Steel, R. Levicky, T. M. Herne and M. J. Tarlov, Electrochemical quantitation of DNA immobilized on gold, *Anal. Chem.*, 1998, **70**, 4670-4677.

32 H. Z. Yu, C. Y. Luo, C. G. Sankar and D. Sen, Voltammetric procedure for examining DNA-modified surfaces: quantitation, cationic binding activity, and electron-transfer kinetics, *Anal. Chem.*, 2003, **75**, 3902-3907.

33 M. Steichen, Y. Decrem, E. Godfroid, C. Buess-Herman, Electrochemical DNA hybridization detection using peptide nucleic acids and $[Ru(NH_3)_6]^{3+}$ on gold electrodes, *Biosens. Bioelectron.*, 2007, **22**, 2237-2243.

34 M. D. Purugganan, C. V. Kumar, N. J. Turro and J. K. Barton, Accelerated electron transfer between metal complexes mediated by DNA, *Science*, 1988, **241**, 1645-1649.

35 R. Wu, G. Ruben, B. Siegel, E. Jay, P. Spielman, C. D Tu, Nucleotide-sequence analysis of DNA. 24. synchronous digestion of SV40 DNA by exonuclease.3., *Biochemistry*, 1976, **15**, 734-740.

36 C. Wu, An exonuclease protection assay reveals heat-shoch element and TATA box DNA-binding proteins in crude nuclear extracts, *Nature*, 1985, **317**, 84-87.

37 J. Hoheisel, On the activities of Escherichia coli Exonuclease III, *Anal. Biochem.*, 1993, **209**, 238-246.

38 S. J. Liu, H. G. Nie, J. H. Jiang, G. L. Shen and R. Q. Yu, Electrochemical sensor for mercury (II) based on conformational switch mediated by interstrand cooperative coordination, *Anal. Chem.*, 2009, **81**, 5724-5730.

39 Z. Lin, X. Li and H. B. Kraatz, Impedimetric immobilized DNA-based sensor for simultaneous detection of Pb^{2+}, Ag^{+}, and Hg^{2+}, *Anal. Chem.,* 2011, **83**, 6896-6901.